2018

CFD Modeling And Performance Evaluation Of A Centrifugal Fan Using A Cut-Cell Method With Automatic Mesh Generation And Adaptive Mesh Refinement

Yanheng Li
Convergent Science, Inc., United States of America, yanheng.li@convergecfd.com

David Henry Rowinski
Convergent Science, Inc., United States of America, david.rowinski@convergecfd.com

Karan Bansal
Convergent Science, Inc., United States of America, karan.bansal@convergecfd.com

Karthik Rudra Reddy
Convergent Science Inc., United States of America, karthik.reddy@convergecfd.com

CFD Modeling And Performance Evaluation Of A Centrifugal Fan Using A Cut-Cell Method With Automatic Mesh Generation And Adaptive Mesh Refinement

Yanheng LI*, David Henry ROWINSKI, Karan BANSAL, Karthik RUDRA REDDY
Convergent Science Inc.,
Madison, Wisconsin, United States

Contact Information (+1-608-230-1552, yanheng.li@convergecfd.com)

* Corresponding Author

ABSTRACT

Computational Fluid Dynamics (CFD) is a convenient and powerful tool for modeling and evaluating the performance of centrifugal compressors, fans, and pumps. Typically, the use of CFD requires significant labor in mesh generation and refinement. Moreover, for rotating transient simulations, a grid-to-grid interface is usually needed to incorporate the rotating impeller. In this work, a finite-volume-based Cartesian cut-cell method is employed to model a centrifugal fan. Both rotating transient simulations and steady steady multiple reference frame (MRF) simulations are analyzed. The cut-cell-based method automatically generates the Cartesian mesh on-the-fly based on the current location of the rotating boundaries, without requiring any grid-grid interface between the rotating part and the stationary part for the rotating transient cases. The grid is also dynamically refined based on the velocity field and y-plus values at the walls. These features greatly save the pre-processing time of the modeling and make it easy for performing global grid convergence studies. The flow is validated against experiment data for both point velocity measurements, and global measurements of mass flow rate and pressure rise. Key simulation parameters and model constants that can affect the global output and local flow details are discussed.

1. INTRODUCTION

Centrifugal fans have extensive application in industries, such as colling blower, drying and air conditioning devices. Computational Fluid Dynamics (CFD) modeling is a powerful tool that offers great insight into the global design performance, local flow structure details, and transient behavior of centrifugal fans. However, the drawback of using CFD in this respect is that it often requires large computational cost and user setup time even given recent rapid advances in computation hardware resources. One of the reason, is that mesh generation is not simple for rotating geometry, and a grid-to-grid interface is usually needed to account for the mesh connectivity between the rotor and the stator. The difficulty in meshing can make it very laborious when investigating the grid dependency in which mesh needs to be revised frequently.

There has been many existing efforts made to investigate the CFD modeling in the analysis of centrifugal fans with non-Cartesian mesh. Petit (2013) studied the ERCOFTAC (European Research Community on Flow Turbulence and Combustion) centrifugal pump local flow details with pre-generated meshes. Reynolds Averaged Navier-Stokes (RANS) turbulence model are adopted by Petit and both the single inertial reference frame approach and the multiple reference frame (MRF) approach are implemented. Zhang et. al. (1996) studied the viscous flow in a three-dimensional centrifugal fan with backwards swept impeller blade using Standard RANS turbulence modeling. Shah et. al. (2010) performed steady state simulation of a centifugal pump with different RANS models for off-design operating conditions and claimed k-omega SST is a better option for turbulence modeling compared with RNG k-epsilon model. Mentzos et. al. (2004) used MRF approach to study the impeller-volute interaction effect but the results were not desirable due to the frozen rotor assumption used in MRF approach. Karanth et. al. (2009) studied the flow behavior within the radial gap between centrifugal fan impeller and diffuser using moving unstructured mesh.

In this work, a finite-volume-based Cartesian cut-cell method is employed to model the ERCOFTAC centrifugal pump [Ubaldi (1996)], which is actually a centrifugal fan with air as the working fluid. Both rotating transient simulations and steady steady multiple reference frame (MRF) simulations are used for global performance and local flow details study. The cut-cell-based method automatically generates the Cartesian mesh on-the-fly based on the current location of the rotating boundaries, without requiring any grid-grid interface between the rotating part and the stationary part for the rotating transient cases. The grid is also dynamically refined based on the velocity field and y-plus values at the walls. These features greatly save the pre-processing time of the modeling and make it easy for performing global grid convergence studies. The flow is validated against experiment data for both local velocity measurements in the diffuser-impeller gap, and global measurements of pressure rise. Key simulation parameters and model constants that can affect the global output and local flow details are discussed. Furthermore, the employed method has its unique advantage in handling general moving geometry which is ubiquitous in pump and compressor applications, and it can greatly save the research and development time while giving promising predictions of the essential physics and performance of many other pump and compressor types, such as screw pumps and reciprocating compressors ([Rowinski(2016)].

2. TEST CASE AND METHODOLOGY

The ERCOFTAC Centrifugal Pump test rig built by Ubaldi et. al. (1996) is used for this study, which uses air as the working fluid and is essentially a centrifugal fan. The device has a 420mm diameter open centrifugal impeller and a vaned diffuser of 644mm diameter. The impeller has 7 backswept blades with constant thickness, and the diffuser has 12 vanes. For this study, the 6% radial gap between the impeller and the diffuser are used and the 0.4mm of tip clearance is adopted [Petit(2013)]. The geometry of the fan is showed in Figure 1(left). For the MRF approach, the rotating reference frame is applied where the diameter is less than 433.8mm in the diffuser-impeller region, shown in Figure 1 (right).

The inlet air temperature is 298K and the air density, ρ, is 1.2kg/m^3. Constant fluid density is used throughout the domain, and the dynamic viscosity, μ, is set at 1.86e-5Pa.s. At the 2000 revolutions per minute rotation rate and the flow rate coefficient of 0.048, the impeller tip speed is U_2= 43.98m/s and the nominal total pressure rise of the device is 754Pa from the suction pipe to the diffuser outlet [Petit(2013)]. Hot wire anemometry and fast-response pressure transducers are used in the original experiment to measure the local point-wise flow quantities and pressure.

The Cartesian cut-cell based second order finite volume algorithm proposed by Senecal et. al. (2007), commercially available as CONVERGE [(Richards et. al. (2017)], is used in this work to solve the Reynolds Averaged Navier-Stokes equation, which has proved its numerical stability and simpleness. A triangulated surface defines the volume of the computational domain, which is filled by orthogonal base grid whose size is predefined by the user. At locations where the surface triangle intersects the base grid, the base cells are cut into partial polyhedra, without moving the vertices of the boundary triangles. Therefore the volume of the original computational domain is precisely preserved in the cut-cell approach regardless of the base grid size. The cell-cutting is implemented on-the-fly based on the current locations of the moving boundaries without user's involvement. The governing equations are solved using finite-volume Pressure Implicit with Splitting of Operators (PISO) method [Issa(1985)] with values collocated at the cell center. Variable time step is used and controlled by local Courant-Friedrichs-Lewy(CFL) numbers. Realizable k-epsilon RANS model are used for turbulence modeling while the effect of different turbulence models are also investigated. The simulations are implemented in parallel with Message Passing Interface (MPI). Automatic Mesh Refinement (AMR) is employed to adaptively refine the mesh based on local sub-grid scale variations, for which the user only have to give the sub-grid criteria before the simulation [Pomraning(2014)]. In this way the grid is only refined where it is necessary, hence it can greatly enhance the overall simulation efficiency.

For the single inertial reference frame approach with a rotating impeller, an incompressible transient solver is used considering the low pressure rise. For the MRF approach, since there are no moving walls in either reference frame, a density-based steady state solver with pseudo time step is used to further improve the simulation efficiency.

No energy transport is solved in this work given the small pressure rise and neglegible wall heat transfer. The algorithm of Rhie and Chow(1983) is used for pressure-velocity coupling to avoid checker-boarding issue among collocated meshes. All cases in this work are run with the realizable k-epsilon RANS turbulence modeling except specifically mentioned. Turbulence kinetic energy intensity of 5% is applied at the inlet and a 0.3mm length scale is provided for turbulent dissipation rate.

The Successive Over-Relaxation(SOR) algorithm is used to solve the momentum equation, while Bi-Conjugate Gradient Stabilized (BiCGSTAB) method is used for pressure equation. At the wall boundary, standard law-of-the-wall models are used for velocity. The inlet is set at atmospheric pressure of 1.01bar while a constant mass flow of 0.351kg/s is applied at the outlet, which corresponds with the nominal flow rate coefficient of 0.048. Note that the system outlet in this work is slightly larger than the diffuser outlet, at 750mm in diameter. The case is first run with very coarse grid (minimum cell size =5mm), then the result from the coarse grid run is used as the initialization for fine grid runs. The steady state solver, starts from large time steps and looser solver tolerances, and gradually the time step is reduced and the tolerances are tightened as it gets closer to the steady state. These algorithms are controlled automatically, without requiring user intervention during runtime.

Figure 1: ERCOFTAC centrifugal fan geometry (left) and MRF region definition(right)

3. Results and Discussion

3.1 Convergence Performance

A typical run with the MRF approach using the steady state solver has a time history shown as Figure 2. In this run, 4.5mm base grid is used with maximum of level 3 refinement, which corresponds with the minimum grid size of $4.5/2^3$=0.5625mm. AMR starts from iteration cycle 2500, and the maximum cell count is 6.3E6. From Figure 2 we can see that the simulation can reach the steady state after 6000 cycles.

Because in the MRF approach, the rotor is not moving in the rotating reference frame, the run time for moving geometry triangles and re-cutting mesh in rotating transient simulation is saved. In addition, larger time-step can be used for MRF approach without undermining the stability compared with the rotating transient simulation. Due to the above reasons, the MRF simulation is more than 5 times faster in achieving a steady state result when starting from the same initial condition as the rotating transient simulation. Owing to the efficiency benefit of MRF approach plus the steady state solver, their combination is ideal for grid convergence and model sensitivity studies.

In order to understand the grid dependency, a series of MRF runs with same model and algorithm parameters but different base grids and refinement level are conducted, where the refinement includes both AMR and boundary mesh refinement. The total pressure rise result with respect to different minimum grid size is shown in Figure 3.

In Figure 3, the total cell count with the coarsest grid is 300,000 with y+~200 at the impeller blade, while the total cell count with the finest grid is 10 million with y+~30 at the impeller blade. From the figure we can see that a desirable grid convergence tendency is shown with given models and algorithms. With a couple of millions of cells, the pressure rise prediction error can fall within the ~5% range of the test value. The capability of the MRF approach to accurately predict the global parameters of this case make it very useful for performance evaluation of the design, which requires to simulate multiple operating conditions.

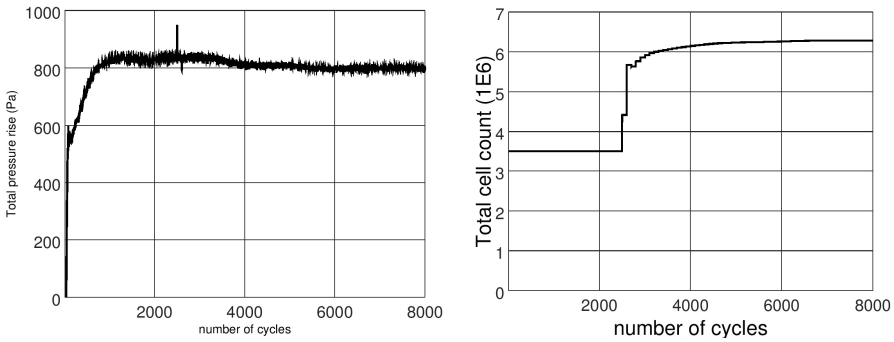

Figure 2: Time history of total pressure rise (left) and total cell (right) counts for a typical MRF run with steady state solver

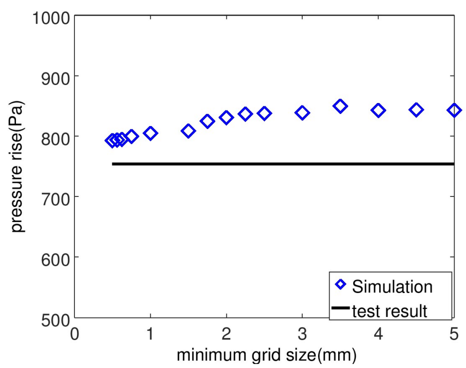

Figure 3: Pressure rise with respect to different minimum grid size (MRF approach).

3.2 Local flow detail predictions

We also investigated the validity of the proposed method in predicting the local flow details. In the original setup there are 107 measuring points mounted at 1.02r_i (224.2mm) of radial location, which is within the gap between the impeller tip and diffuser vane. In our simulation, monitor points with output for local velocity component are also set up to get the time history of velocities at the locations of interest. Three runs are conducted for both the MRF approach and the rotating transient approach with different grid sizes, with the tangential and radial velocity profile at blade midspan shown in Figure 4. The minimum grid size in the fine grid case is 0.625mm, 0.75mm for the medium grid case, and 0.875mm for the coarse grid case. From Figure 4 we can see that the MRF approach can well capture the peaks of the tangential velocity which correspond to the maximum wake near the impeller blade tip, although there is a slight phase lag (~5 degree) compared with the test value. The overall trend of U_r along the tangential direction is also well represented with slight underestimation in magnitude. When comparing with the rotating transient simulation in Figure 4 bottom left and bottom right, MRF approach has similar performance in predicting the local flow near the impeller-diffuser gap with smaller phase lag. It is also demonstrated that, for both MRF approach and rotating transient approach, the local flow prediction is not significantly affected by the grid size when reasonable grid resolution (y+<~100) is achieved.

However, the MRF approach does have its limitations. The local flow velocity profile in Figure 4 is measured within the rotating reference frame. For regions near and outside interface for inertial and rotating reference frame, the momentum conservation assumption across the interface will produce non-physical wakes when compared with rotating transient simulation, shown as in Figure 5. From the left side of Figure 5 we can see that for the rotating transient simulation, the impeller tip wake naturally follows the motion of the impeller, which is the realistic case; while in the right side of Figure 5 we can see, for the MRF approach, there is a sudden change in velocity contour across the interface. This is a common issue of MRF approach as addressed by many researchers, such as Petit(2013) and Mentzos(2010). The resulting artificial wakes can cause problems if there is strong interaction between the impeller and the volute. Additionally, the frozen rotor assumption used by the MRF approach is not suitable in handling transient behavior study such as flow surge.

3.3 Other effects

For the presented cut-cell based method, the overall simulation benefits greatly from the use of AMR. For example, given two MRF simulations with the same total cell count of ~6E6, one case has no AMR but with a maximum level 2 refinement near the wall, and another case has velocity AMR throughout the domain with maximum level 2 refinement. The case with AMR converges to the steady state after 6000 cycles while the one without AMR still not well converged after 10000 cycles. And the one with AMR gets a closer pressure rise prediction than the one without (797Pa with AMR, 822Pa without AMR and 754Pa experiment). The comparison is shown in Figure 6. Model and geometry sensitivities are also investigated in this work. It is found that the surface roughness with absolute high less than 5e-5m (which is as the same order for stainless steel) does not have significant effect on the results, only slightly affecting the global pressure rise. The leakage through the clearance between the diffuser blade and the casing also only has a very small effect on global pressure rise. But turbulence models do have considerable impact on the global parameters. Four runs with same grid but different turbulence models are conducted, including realizable k-epsilon, RNG k-epsilon, SST k-omega, and no turbulence modeling. The time history and pressure rise results from each run is shown in Figure 7 and Table 1. The total cell count for all cases is 6 million. It can be seen that realizable k-epsilon model predicts best result among all RANS models. While no tubulence modeling yields even better predictions, this choice is not justified as the y+ near the wall is not small enough (>30).

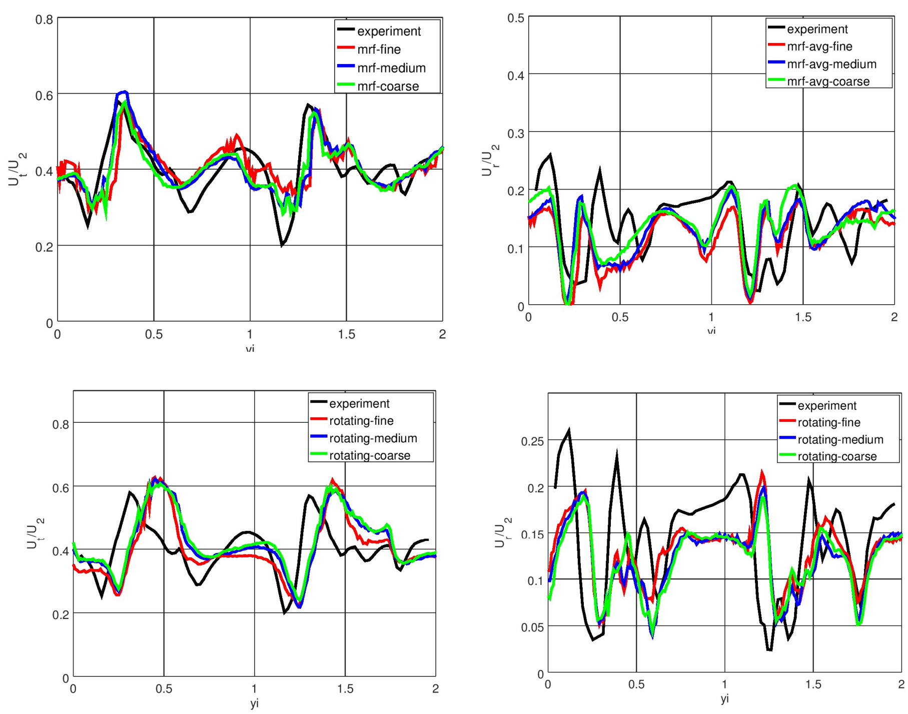

Figure 4: Local relative tangential and radial velocity distribution across two blade spans at d=428.4mm). y_i represents the circumferential coordinates in the unit of impeller blade span, the velocity is is normalized by impeller tip speed U_2. The top left and right is tangential velocity profile and radial velocity profile for MRF approach and the bottom left and right is tangential and radial velocity profile for rotating transient approach.

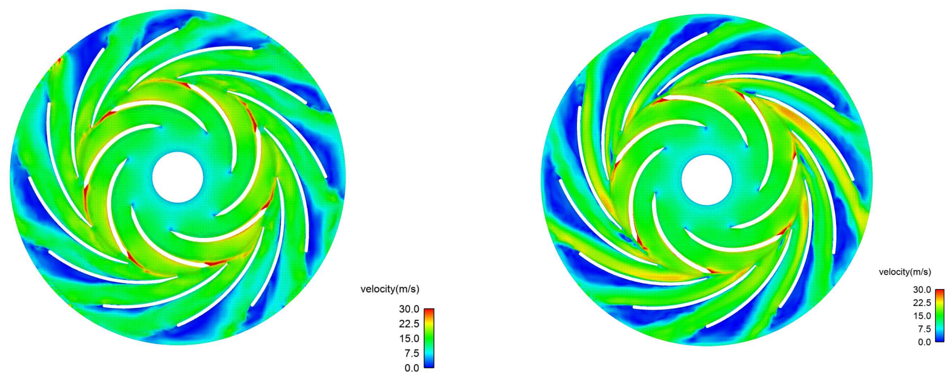

Figure 5: Velocity contour of rotating transient approach (left)and MRF approach (right)

Table 1: Turbulence Effect on the pressure rise

Turbulence Model	Realizable k-eps.	RNG k-eps.	SST k-omega	No turbulence
Pressure Rise(Pa)	797	825	811	782

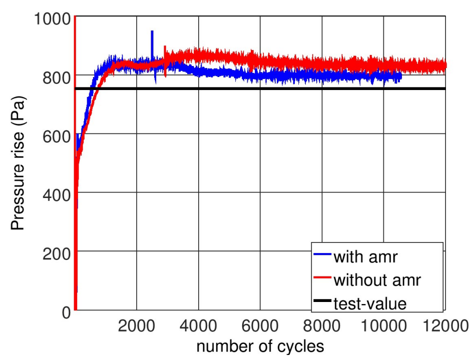

Figure 6: Pressure rise time history comparison between case with AMR and case without AMR

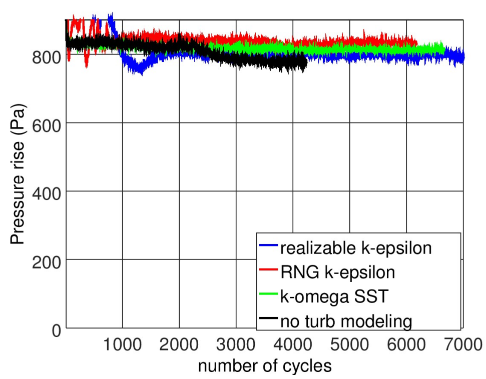

Figure 7: Pressure rise results from different turbulence models

4. CONCLUSIONS

In this study, we investigated the validity and accuracy of a Cartesian cut-cell based finite-volume method applied to a centrifugal fan. The proposed method greatly mitigates the mesh-generation difficulty for applications with rotating boundaries, with the capability of generating a high quality stationary orthogonal cut-cell mesh and mesh refining on-the-fly. Both an MRF approach with a steady state solver and a rotating approach with a transient solver are used. By showing the global pressure rise and local flow details with respect to different grids, it is demonstrated that the proposed MRF approach in combination with steady state solver has agreeable accuracy in predicting both global and local quantities.

Compared with the moving transient simulation, the MRF approach does not have moving boundaries, hence avoiding re-generating the mesh for each time step. And it also allows a larger time step due to the frozen rotor assumption. These benefits determine that the MRF approach is much more efficient than the rotating transient approach, making it a good choice when studying the grid dependency or evaluating multiple operating conditions. However, the MRF approach will inevitably produce un-physical wakes near and outside the interface between the rotating frame and the inertial frame, which make it not as desirable as the rotating transient approach to study the impeller-volute interaction effect and other transient behaviors.

The benefit of AMR is also demonstrated in this work, which is both more efficient and more accurate compared with runs without AMR. Also, in the selected ERCOFTAC centrifugal fan case, the realizable k-epsilon RANS model is shown to have better predictions compared with other RANS based turbulence models. Although the result from without turbulence modeling is even closer to the test value, the y+ value at the impeller is not small enough to justify the boundary layer resolution.

REFERENCES

Issa, R. I. (1985). Solution of the Implicitly Discretised Fluid Flow Equations by Operator-Splitting. *Journal of Computational Physics*, 62.

Karanth, K.V., Sharma, N.Y. (2009). CFD Analysis on the Effect of Radial Gap on Impeller-Diffuser Flow Interaction as well as on the Flow Characteristics of a Centrifugal Fan. International Journal of Rotating Machinery, 2009-293508.

Mentzos, M., Filios, A., Margaris, P., Papanikas, D. (2004). A Numerical Simulation of the Impeller-Volute interaction in a Centrifugal Pump. Proceedings of International Conference from Scientific Computing to Computational Engineering. Pp. 1-7.

Petit, O., Nilsson, H. (2013). Numerical Investigation of Unsteady Flow in a Centrifugal Pump with a Vaned Diffuser. International Journal of Rotating Machinery, 2013-961580.

Pomraning, E., Richards, K., and Senecal, P. (2014). Modeling Turbulent Combustion Using a RANS Model, Detailed Chemistry, and Adaptive Mesh Refinement. *SAE Technical Paper 2014-01-1116.*

Rhie, C. M. and Chow, W. L. (1983). Numerical Study of the Turbulent Flow Past an Airfoil with Trailing Edge Separation.AIAA J., 21, 1525-1532.

Richards, K. J., Senecal, P. K., Pomraning, E. (2017). CONVERGE 2.4 Manual, Convergent Science Inc., Madison, WI.

Rowinski, D. H. and Davis, K. E. (2016). Modleing Reciprocating Compressors Using A Cartesian Cut-Cell Method With Automatic Mesh Generation. International Compressor Engineering Conference.

Senecal, P. K., Pomraning, E., Richards, K. J., Briggs, T. E., Choi, C. Y., McDavid, R. M., Patterson, M. A., Hou, S., & Shethaji, T. (2007). A New Parallel Cut-Cell Cartesian CFD Code for Rapid Grid Generation Applied to In-Cylinder Diesel Engine Simulations. SAE Technical Paper, #2007-01-0159.

Shah, S., Jain, S., Lakhera, V. (2010). CFD Based Flow Analysis of Centrifugal Pump. Proceedings of International Conference on Fluid Mechanics and Fluid Power, #TM08.

Ubaldi, M., Zunino, P., Barigozzi, G. and Cattanei, A. (1996). An Experimental Investigation of Stator Induced Unsteadiness on Centrifugal impeller outflow," Journal of Turbomachinery, vol. 118, no. 1, pp. 41–51.

Zhang, M. J., Pomfret M. J., Wong C. M. (1996). Three-dimensional Viscous Flow Simulation in a Backswept Centrifugal Impeller at the Design Point. Computers and Fluids, 25(5).